studies reported acute infantile encephalopathy predominantly affecting the frontal lobes and acute encephalopathy with biphasic seizures and late reduced diffusion (AESD) in non-Japanese patients; therefore, it seems that this clinical entity is not limited to the Japanese population [2,3]. Acute encephalopathy is typically characterized by a biphasic clinical course. It usually begins with status epilepticus and a mild symptomatic period of 2–3 days, followed by a cluster of seizures accompanied by a decreased level of consciousness. During this period, diffusion-weighted images obtained by magnetic resonance imaging (MRI) show strong signal intensities in the subcortical regions, referred to as BTA [1]. Few atypical types of acute encephalopathy with BTA have been described, including cases with altered consciousness but no status epilepticus or cases with a monophasic clinical course [4,5]. No standard treatment has been described for this entity, although glutamatergic excitotoxicity was proposed as its main pathomechanism [6]. Sequelae may include mild to severe motor and intellectual disability and epilepsy. The prognostic factors for acute encephalopathies, including one case with BTA, have been reported as a decrease in platelet count; an increase in aspartate aminotransferase (AST), alanine aminotransferase (ALT), creatine kinase (CK), lactate dehydrogenase (LDH), and creatinine (Cr) levels; and abnormal blood sugar levels and clotting times [5,7,8]. Here we retrospectively examined the prognostic values of several serum markers, changes in these markers during the acute stage, and the findings of magnetic resonance spectroscopy (MRS) of the BTA lesion during the BTA period.

2. Methods

The participants included 10 patients with acute encephalopathy and BTA who were admitted to Osaka University Hospital from 2003 to 2012. Eight of the patients presented with fever and status epilepticus, which continued for over 30 min on day 0. MRS confirmed the presence of BTA from the 3rd to the 9th day of the illness. The other 2 patients did not present an obvious convulsive event; however, 1 of them presented with loss of consciousness, and BTA was confirmed in this patient on the 6th day. The other patient was transferred to the emergency room with loss of consciousness and respiratory arrest, and BTA was confirmed on the 8th day. For the 10 participants, we retrospectively examined the clinical history, clinical features, changes in different serum marker levels, and brain MRI findings.

Evaluation of clinical history included the patient's underlying condition, any past history of febrile convulsions, neurological status before encephalopathy, type of infectious disease, existence of a biphasic course, length of the latency period between fever onset and encephalopathic episode onset, duration of primary status epilepticus, specific medication used to cease convulsions and sedate, use of any prescribed antiepileptic agents during the acute phase, and history of specific treatment for acute encephalopathy. Neurological outcome was evaluated 1 year after the onset of encephalopathy. The intelligence or development quotient was not accurately estimated by developmental tests in most patients. Therefore, the severity of cognitive impairment was estimated and classified as follows: normal or mild if the patient could utter some meaningful words (for patients aged 12–24 months) or have a simple conversation (for patients aged >24 months), moderate if a patient could utter a few meaningful words (for patients aged >24 months), and severe if a patient could not utter meaningful words. For patients aged >12 months, the severity of motor impairment (MI) was estimated and classified as follows: normal or mild if the patient could walk without support, moderate if the patient could sit without support but not walk without support, and severe if the patient could not sit without support. The neurological status of patient 6, who presented with an underlying disease before encephalopathy, was not evaluated according to these criteria because the patient was aged <12 months. This patient could babble and hold the head upright but could not turn over unassisted before encephalopathy. We estimated that the patient had moderate mental retardation (MR) and MI. We divided patients into 2 groups according to the severity of encephalopathy, namely severe and mild groups, on the basis of the patient's neurological status at 1 year after the onset of encephalopathy. The mild group included patients with mild cognitive and/or mild motor impairment. The severe group included patients with a more severe neurological impairment. Therefore, 6 patients were included in the severe group and 4 patients in the mild group.

Blood samples were obtained during convulsions, immediately after the end of convulsions, or immediately after arrival at the hospital for patients without convulsions. We investigated the maximum and minimum values and any changes observed during the first 20 days in several serum marker levels. These markers included blood cell counts and AST, ALT, LDH, CK, blood urea nitrogen (BUN), Cr, sodium, potassium, chloride, total protein content, albumin, and blood sugar levels.

Brain imaging findings for the acute phase and chronic phase were examined >7 months later by performing MRI using a 1.5T Signa HD (GE Healthcare, Milwaukee, WI) system with a standard head coil. MRS [point-resolved spectroscopy sequence (PRESS): repetition time/echo time, 1800/136] was subsequently performed on BTA detection, and the region of interest was marked on the BTA lesion. Model information and condition of acquisition was not confirmed in patients 2 and 6. On MRS, we examined the peak of lactate and

Table 1
Clinical features of the patients.

Patient	Age	Sex	Underlying disease	History of FS	Neurological status before encephalopathy	Initial symptom	Infection	Biphasic clinical course	Antiepileptic drugs for the acute phase	Therapy for the acute phase	Outcome
1	6 y	M	No	Yes	Normal	Impaired consciousness	Influenza A	No	MDL, PB	mPSL	Epilepsy, moderate MI, severe MR
2	5 y	M	Klinefelter syndrome	Yes	Epilepsy Mild MI Mild MR	Status epilepticus	Influenza A	No	DZP, PB	mPSL, IVIG	Epilepsy, severe MI severe MR
3	4 y	M	Psychomotor retardation	Yes	Mild MI Mild MR	Status epilepticus	Unknown	No	MDL, thiopental, thiamilal, PB	mPSL, IVIG	Epilepsy, severe MI, severe MR
4	2 y	M	Chromosomal abnormality	No	Moderate MI Moderate MR	Status epilepticus	Influenza A	No	DZP, MDL, LDC, PB, PHT	mPSL, IVIG	Epilepsy, severe MI, severe MR
5	1 y	F	No	No	Normal	Status epilepticus	HHV6	Yes	MDL, thiopental, LDC, PB	mPSL	Epilepsy, moderate MI, severe MR
6	6 m	M	Kabuki syndrome	No	Moderate MI Moderate MR	Status epilepticus	Unknown	No	DZP, MDL, thiopental, PB, PHT	mPSL, IVIG	Epilepsy, severe MI, severe MR
7	4 y	F	Costello syndrome	Yes	Epilepsy Mild MR	Status epilepticus	Influenza A	Yes	DZP, MDL, PB	mPSL	Epilepsy Mild MR
8	2 y	M	No	No	Normal	Impaired consciousness	Adenovirus type3	Yes	MDL, PB	mPSL	Mild MR
9	2 y	F	No	No	Normal	Status epilepticus	Unknown	No	DZP, MDL, PB	mPSL, IVIG	Mild MR
10	1 y	M	Cerebral Palsy	Yes	Mild MI Mild MR	Status epilepticus	Influenza A	No	DZP, MDL, thiamilal, PB	mPSL	Mild MI Mild MR

DZP: diazepam, MDL: midazolam, LDC: lidocaine, PB: phenobarbital, PHT: phenytoin, mPSL: methylprednisolone, IVIG: intravenous immunoglobulin, MR: mental retardation, MI: motor impairment, FS: febrile seizures, M: male, F: female, y: year, m: month.
Patients 1–6 belong to the severe group, while patients 7–10 belonged to the mild group.

the ratio of N-acetyl aspartic acid and creatine + phosphocreatine (NAA/Cr).

Statistical analyses were performed using JMP 8.0 statistical software (SAS Institute Inc., Cary, NC, USA) and the Mann–Whitney *U* test was used to test for significant differences between the severe and mild groups. Statistical significance was determined at $p < 0.05$.

3. Results

3.1. Clinical features

The total observation period was 7 months to 9 years. The latency period from fever onset to seizures or state of altered consciousness was <24 h in all patients. The age of onset ranged from 6 months to 6 years (median, 3 years) in the severe group and from 1 year to 4 years (median, 3 years) in the mild group. No significant difference in age was observed between the 2 groups ($p = 0.587$). Six of the 10 patients presented some underlying condition. The duration of status epilepticus ranged from 40 to 60 min (median, 50 min) in the severe group and 40–50 min (median, 45 min) in the mild group. No significant difference in duration was observed between the 2 groups ($p = 0.362$). Thiopental or thiamilal was required to cease convulsions in addition to the initially administered diazepam (DZP) or midazolam (MDL) in 5 patients in the severe group; DZP alone was sufficient for 2 patients in the mild group. Two patients without evident convulsions developed respiratory or cardiopulmonary arrest on arrival, and resuscitation was performed in the emergency room. These patients were placed on respirators and received continuous infusions of MDL during the acute phase. All patients were treated by methylprednisolone pulse therapy. Intravenous immunoglobulin (IVIG) was administered to 4 patients in the severe group and 1 patient in the mild group (Table 1).

Neurological sequelae included epilepsy or severe MI in addition to regression in the severe group. The neurological status of the 4 patients with underlying disease in the severe group had been stable before encephalopathy. However, their status evidently worsened after

encephalopathy. Mild MR was observed in all patients in the mild group; however, 2 patients with underlying disease had mild MR before encephalopathy (Table 1).

3.2. Serum markers

Seven out of the 10 patients studied showed maximum values of AST and ALT within 10 days of admission, and all patients showed maximum values of LDH and CK within 10 days. These markers returned to normal levels approximately 1 month later (Table 2). The maximum LDH values observed in the severe group were higher than those in the mild group, but that difference was only marginally significant ($p = 0.055$). The platelet counts reached the minimum value between the first and fourth day of hospitalization and returned to normal levels shortly thereafter (Fig. 1). The

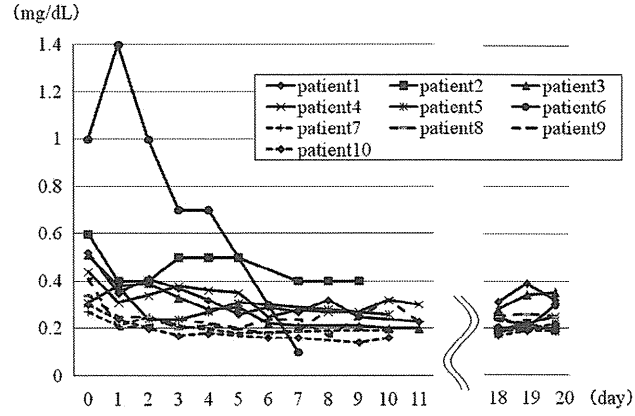

Fig. 2. Change in serum Cr levels, Cr: creatinine. The solid line represents the severe group (patients 1–6), and the dotted line represents the mild group (patients 7–10).

Table 2
Comparison of serum markers between the severe and mild groups.

		Severe group ($n = 6$)		Mild group ($n = 4$)		p Value
		Median (range)		Median (range)		
Maximal AST	(IU/L)	600	(220–1341)	372	(114–719)	0.2
Maximal ALT	(IU/L)	253	(132–1350)	162	(49–373)	0.2864
Maximal CK	(IU/L)	1247	(572–4723)	281	(141–524)	0.1356
Maximal LDH	(IU/L)	1204	(1018–5211)	875	(655–1057)	0.055
Maximal Cr	(mg/dL)	0.515	(0.44–0.6)	0.32	(0.285–0.375)	0.019*
Cr in the convalescent phase	(mg/dL)	0.24	(0.19–0.3)	0.21	(0.18–0.24)	0.3359
Maximal BS	(mg/dL)	219	(176–252)	311	(118–411)	0.3938
Minimal Plt	($\times 10^3/\mu L$)	9.4	(9.1–10)	20	(17.5–22.5)	0.0325*

AST: aspartate aminotransferase, ALT: alanine aminotransferase, CK: creatine kinase, LDH: lactate dehydrogenase, Cr: creatinine, BS: blood sugar, Plt: platelet.
Statistical analysis was performed using the Mann–Whitney U test.
* $p < 0.05$.

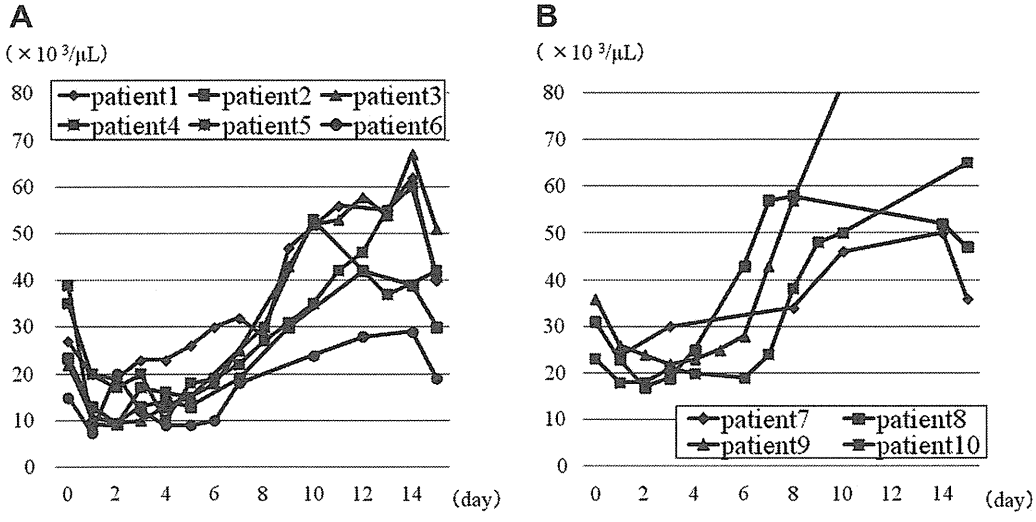

Fig. 1. Change in platelet counts. (A) Severe group, (B) mild group.

Table 3
Maximum Cr values and urine volume in the acute phase and Cr values in the convalescent phase.

Patient	Maximal Cr levels in the acute phase (mg/dL)	Cr levels, 97.5% (mg/dL)	Urine volume on day 0 (mL/kg/h)	Cr levels in the convalescent phase (mg/dL)
1	0.52	0.48	4.66	0.31
2	0.6	0.45	1.47	0.3
3	0.51	0.4	2.35	0.28
4	0.44	0.37	1.18	0.18
5	0.38	0.32	Not measured	0.19
6	1.4	0.31	4.52	0.2
7	0.27	0.4	Not measured	0.19
8	0.34	0.37	6.5	0.23
9	0.41	0.37	3.94	0.25
10	0.3	0.32	3.67	0.17

Cr: creatinine.
Cr 97.5%: 97.5 percentile value in age-matched Japanese children.

minimum platelet count was significantly lower in the severe group than in the mild group ($p < 0.05$). The maximum Cr value was observed on the day of onset or the following day in all patients (Fig. 2, Table 3); however, that maximum value was significantly higher in the severe group than in the mild group ($p < 0.05$). During the first week of illness, the Cr value was higher in the severe group than in the mild group, and no significant difference was observed between the 2 groups on the 20th day ($p = 0.336$). No significant differences were observed in any of the other markers between the 2 groups (Table 2).

3.3. Brain MRI and MRS

The median period of time elapsed between hospital admission and confirmation of the presence of BTA was 7 days. BTA was observed in different regions, with 2 patients in the mild group showing global involvement with spared pericentral areas. MRI performed during the chronic phase showed severe brain atrophy in all patients in the severe group, which was absent before encephalopathy, and mild to intermediate atrophy in all patients in the mild group (Table 4). None of the patients presented any thalamic lesions, diffuse brain edema, or hernia compressing the brain stem throughout the clinical course.

MRS was performed for 9 patients during the BTA period. A lactate peak was observed in 5 out of the 6 patients included in the severe group and 1 out of the 3 patients in the mild group (Fig. 3). In the mild group, the only patient presenting a lactate peak also showed intermediate cerebral atrophy during the remote period, while the 2 patients without a lactate peak showed only mild atrophy. The NAA/Cr ratio was 0.88–1.34 (median, 0.97) in the severe group and 1.13–1.19 (median, 1.17) in the mild group. No significant differences were observed between the 2 groups ($p = 0.178$; Table 4).

4. Discussion

Hayakawa proposed the integration of the 3 most common acute encephalopathies in Japan (namely, acute encephalopathy with febrile convulsive status epilepticus or AEFCES, AESD, and acute encephalopathy with biphasic clinical course) into one type of encephalopathy because of the overlap in clinical features and similarities in pathomechanisms. However, he reported that only 36% patients experienced all the symptoms in the triad: BTA, status epilepticus at illness onset, and biphasic clinical course [4]. Hayashi defined acute encephalopathy with reduced diffusion (AED), which encompasses a spectrum that includes not only typical AESD but also atypical AESD with a monophasic

Table 4
Findings of brain MRI and MRS.

Patient	Brain MRI (acute phase)			Brain MRI (chronic phase)
	Position of BTA	MRS:lactate peak	MRS:NAA/Cr	
1	Whole brain	(+)	0.88	Severe atrophy
2	Whole brain	(+)	0.98	Severe atrophy
3	Whole brain	(+)	0.97	Severe atrophy
4	Bioccipital lobe predominant	(+)	0.48	Severe atrophy
5	Right hemisphere	(−)	1.34	Severe atrophy of right hemisphere
6	Bifrontal lobe predominant	(+)	No data	Severe atrophy
7	Right hemisphere	(−)	1.19	Mild atrophy of right hemisphere
8	Whole brain (central sparing)	Not done	Not done	Moderate atrophy
9	Bioccipital lobe predominant	(−)	1.17	Mild atrophy
10	Whole brain (central sparing)	(+)	1.13	Moderate atrophy

BTA: bright tree appearance, MRI: magnetic resonance imaging, MRS: MR spectroscopy.
MRS was performed by a point-resolved spectroscopy sequence (PRESS).
Echo time (TE)/repetition time (TR) = 1800/136.
NAA: N-acetyl aspartic acid.
Cr: creatine + phosphocreatine.

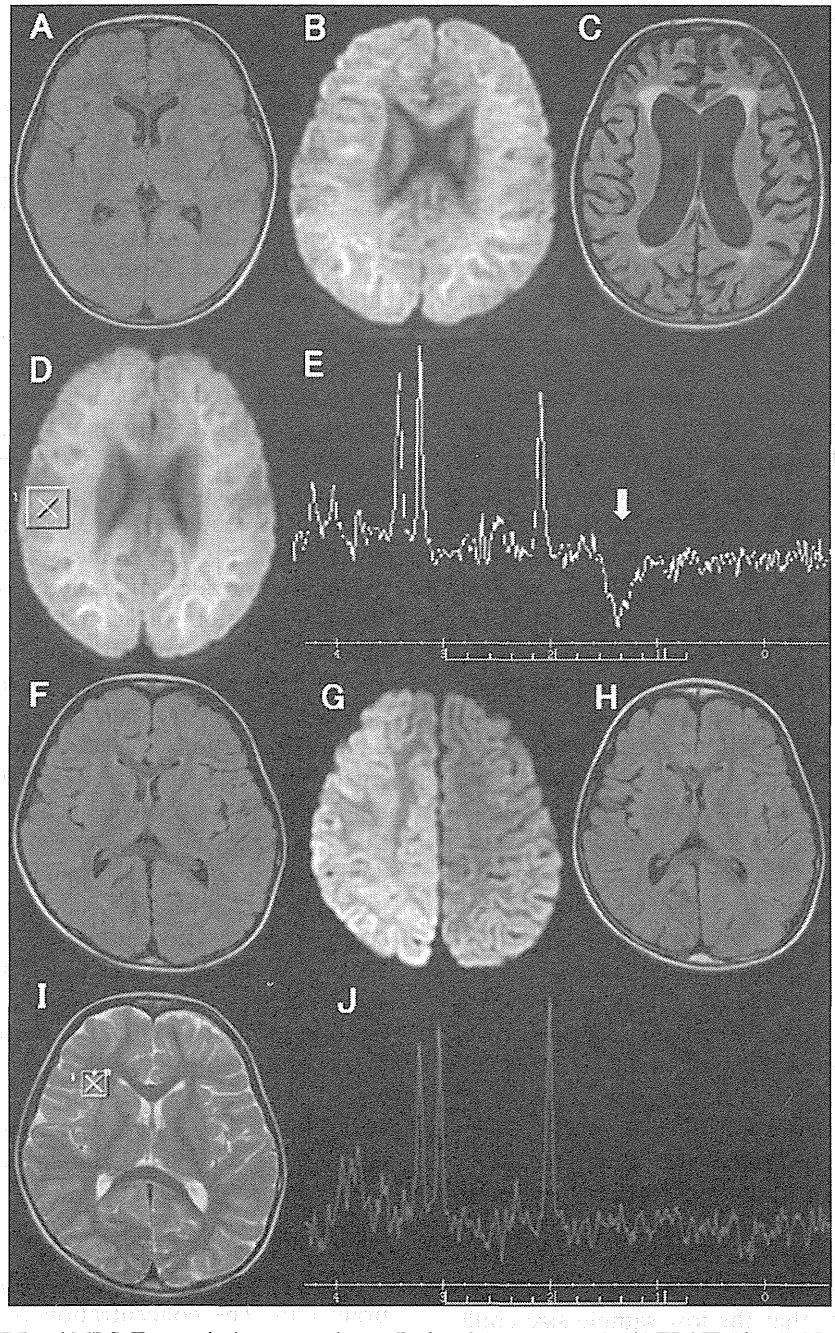

Fig. 3. Findings of brain MRI and MRS. Two typical cases are shown. Patient 3 (severe group). (A) FLAIR (day 1): No abnormal lesion is observed. (B) Diffusion-weighted imaging (DWI; day 6): Abnormal high intensities are observed in the whole subcortical white matter. (C) FLAIR (3 years later): Diffuse cerebral atrophy is observed. (D) Region of interest (ROI) on MRS. (E) MRS (point-resolved spectroscopy sequence (PRESS): repetition time (TR)/echo time (TE), 1800/136) shows a lactate peak. The arrow indicates the lactate peak. Patient 7 (mild group). (F) FLAIR (day 1): No abnormal lesion is observed. (G) DWI (day 6): Abnormal high intensities are observed in the right hemispheric cortical and subcortical white matter. (H) FLAIR (1 year later): Cerebral atrophy was observed in the right hemisphere. (I) ROI of MRS. (J) MRS (PRESS: TE/TR, 1800/136) shows no lactate peak. MRI: magnetic resonance imaging MRS: MR spectroscopy FLAIR: fluid-attenuated inversion recovery.

clinical course, or more severe subtypes [5]. In our study, only 3 patients showed a biphasic clinical course. However, it is worth pointing out that the other patients were treated with antiepileptic agents immediately after the onset of status epilepticus. We diagnosed 8 patients with AED, but we could not categorize 2 patients who presented with altered consciousness but no seizures at onset. In the present study, regardless of the clinical symptoms, all patients presented with BTA and some similitudes in laboratory data, including maximum LDH and CK values within 10 days, minimum platelet counts within the 1st–4th days, and maximum Cr values on the day of onset or following day. Therefore, we could assume a similar pathophysiology for all patients.

We also considered patients with BTA from the 3rd to 9th days as cases of acute encephalopathy with BTA. Overexpression of glutamate, abnormal increase in intracellular calcium ion levels, and subsequent neuronal cell death can be suggested as the possible pathomechanisms behind this encephalopathy. Takanashi reported an association between the appearance of a glutamine/glutamate complex peak on MRS during the BTA period and delayed neuronal cell death [6]. In our study, cases that showed a lactate peak displayed severe brain atrophy and subsequent severe neurological sequelae. To the best of our knowledge, this is the first study reporting the appearance of a lactate peak during the BTA period. A lactate peak on MRS generally reflects an elevation in anaerobic glycolysis or a disorder in aerobic glycolysis; therefore, it appears during the acute phase of an ischemic brain injury [9]; hypoxia [10]; a disorder of the tricarboxylic acid cycle, such as a mitochondrial disease [11]; and a state of imbalance between energy supply and demand, such as brain tumor [12]. We believe that energy failure may have led to neuronal necrosis and severe brain atrophy during the remote period in patients presenting the lactate peak.

In neural cells, NAA is synthesized from acetyl CoA and aspartate through L-aspartate N-acetyltransferase. The Cr peak observed on MRS comprised both Cr and phosphocreatine. The Cr peak is known to be stable; therefore, it is frequently used as the standard for other chemicals [13,14]. During the acute phase of brain infarction, the lactate peak appears immediately after onset; however, the Cr peak does not change within the first 24 h after onset. Therefore, it is believed that the NAA/Cr ratio reflects the metabolic rate of the neural cells and axons, while a decrease in NAA/Cr reflects the decrease or dysfunction in neural cells. Aaen et al. reported a decrease in NAA/Cr and the appearance of lactate peaks in patients with severe brain traumatic injury [15]. In the present study, no significant difference was observed between the mild and severe groups, although we considered that the NAA/Cr tended to be lower in the severe group. Nevertheless, we cannot underestimate the effect that the low sample size could have in these results.

Hayashi reported that AST, LDH, and CK levels reached a maximum value within 10 days from the onset of the illness and that they were significantly higher in the severe group [5]. Ishii reported an abrupt increase in neuron-specific enolase in all patients during the 2nd period (mean, 85.4 ± 40.6 ng/μL), and these high values were maintained for a month before they gradually decreased [16]. Ishikawa proposed that the presence of a high initial serum Cr value could be a useful marker to differentially diagnose prolonged febrile convulsions and AEFCES. On the other hand, they could not identify the reason for the increase of Cr levels, and no renal failure was observed [17]. The changes in serum markers detected in this study were similar to those reported by the abovementioned previous studies. Serum Cr levels showed the highest values either on the day of onset or the following day, and platelet counts showed the lowest values at some point between the 1st and 4th days. Within 10 days after the onset of the illness, 7 of the 10 patients presented their highest values of AST and ALT, and all patients displayed their highest values of LDH and CK. However, the reason behind the correlation between poor prognosis and increased LDH levels and a significant decrease in platelet counts remains unclear.

Five out of the 6 patients in the severe group had serum Cr levels higher than the 97.5 percentile of age-matched controls in their initial measurements; the remaining patient also had a value markedly higher than the 97.5 percentile of age-matched controls by the following day [18]. Their values were higher than the values during the convalescent period around the 20th day. The primary symptom of acute kidney injury is oliguria or anuria. The increase in serum Cr levels reflects the decrease in Cr clearance. Waikar reported that in patients with a >50% decrease in Cr clearance, a 50% increase in serum Cr levels is reached in 12–48 h [19]. Eight out of the 10 patients received urinary catheters, and the urine volume was accurately measured to ensure that the urine volume remained constant. Therefore, we could conclude that these patients did not have acute kidney injury during the acute phase. The increase in serum Cr levels may thus reflect a neurological dysfunction, given that these increased levels also correlate with the incidence of neurological sequelae.

Cr is the last product of creatine metabolism. Creatine is produced primarily in the liver, kidney, and pancreas and is stored in the skeletal muscle as phosphocreatine. Phosphocreatine plays an important role for buffering energy and is essential for the ATP-generating reaction:

$$\text{ADP} + \text{phosphocreatine} \leftrightarrow \text{ATP} + \text{creatine}$$

This energy-buffering mechanism also exists in the brain [20]. The concentration of creatine in the brain is approximately 200-fold higher than that in the serum [21], with the brain presenting the second highest concentration of creatine after the skeletal muscle. Creatine in the brain is directly supplied from the circulatory system through the blood–brain barrier and through production within astrocytes [20]. It is stored in the brain as phosphocreatine and converted to creatine by the brain isozyme for creatine kinase. Creatine is ultimately converted to Cr and released into the blood vessels through the blood–cerebrospinal fluid barrier [22].

Two possible mechanisms may explain the higher Cr value detected in the severe group. The more severe destruction of the blood–cerebrospinal fluid barrier in

the severe group may lead to the flood of Cr. Overproduction and leakage of Cr, synthesized by the phosphocreatine–creatine reaction facilitated by the energy demand in acute encephalopathy, can also explain the higher Cr values. Kubota reported a significant decrease in serum ATP levels during the acute phase of acute encephalopathy compared with the levels detected during the convalescent phase and ascribed it to mitochondrial dysfunction [23]. Although energy expenditure increases tremendously during the acute phase of acute encephalopathy, the production and supply of ATP cannot satisfy the demand, leading to ATP shortage. Although this hypothesis needs to be verified, all patients in the severe group showed significantly higher serum Cr values on the day of onset or the following day. This information may help in differentiating severe from mild cases, even in the early phase of the disease.

A disorder of cytokine secretion is not the main pathomechanism in acute encephalopathy with BTA [24]. In fact, it has been suggested that methyl prednisolone pulse therapy or IVIG therapy are not effective for this encephalopathy. Alternative promising therapies include cerebral hypothermia, edaravone, cyclosporine, high-dose antithrombin, and hemodialysis. The efficacy of cerebral hypothermia has been reported in patients with febrile convulsive status epilepticus [25], neonatal hypoxic ischemic encephalopathy [26], and encephalopathy after resuscitation in adults [27]. The mechanism of cerebral protection in cerebral hypothermia is assumed to be the inhibition of glutamate release [28]. Therefore, it is believed that cerebral hypothermia can be effective against acute encephalopathy with BTA, which leads to delayed neuronal cell death through the over-release of glutamate. However, the therapeutic time window to use cerebral hypothermia is reportedly only a few hours after the onset of the illness [29]. Cerebral hypothermia performed earlier with the detection of increase in serum Cr levels on the day of onset or the following day, rather than with the detection of BTA from the 3rd to 7th days, may lead to a better prognosis. In conclusion, serum Cr levels on the day of onset or the following day, minimum platelet count during the first 4 days, and a lactate peak in the BTA lesion on MRS were significant predictors of poor prognosis. Among these, the initial serum Cr level is expected to be an excellent predictor of prognosis in the acute phase.

References

[1] Shiomi M, Ishikawa J, Yoshimoto A, Togawa M, Kuki I, Okazaki S, et al. Clinical characteristics of acute encephalopathy with febrile convulsive status epileptics (in Japanese). No To Hattatsu 2005;37(Suppl.):166.

[2] Jequier Gygax M, Deonna T, Maeder P, Mayor-Dubois C, Roulet-Perez E. Acute infantile encephalopathy predominantly affecting the frontal lobe (AIEF): a European case. Eur J Paediatr Neurol 2011;15:158–62.

[3] Yadav SS, Lawande MA, Kulkarni SD, Patkar DA. Acute encephalopathy with biphasic seizures and late reduced diffusion. J Pediatr Neurosci 2013;8:64–6.

[4] Hayakawa F. Development of ABC classification of acute encephalopathy in Japan (in Japanese). Shouni Naika (Tokyo) 2013;45:195–200.

[5] Hayashi N, Okumura A, Kubota T, Tsuji T, Kidokoro H, Fukasawa T, et al. Prognostic factors in acute encephalopathy with reduced subcortical diffusion. Brain Dev 2012;34:632–9.

[6] Takanashi J, Tada H, Terada H, Barkovich AJ. Excitotoxicity in acute encephalopathy with biphasic seizures and late reduced diffusion. AJNR Am J Neuroradiol 2009;30:132–5.

[7] Nagao T, Morishima T, Kimura H, Yokota S, Yamashita N, Ichiyama T, et al. Prognostic factors in influenza-associated encephalopathy. Pediatr Infect Dis J 2008;27:384–9.

[8] Morita H, Hosoya M, Kato A, Kawasaki Y, Suzuki H. Laboratory characteristics of acute encephalopathy with multiple organ dysfunctions. Brain Dev 2005;27:477–82.

[9] Rehncrona S, Rosen I, Siesjo BK. Brain lactic acidosis and ischemic cell damage: 1. Biochemistry and neurophysiology. J Cereb Blood Flow Metab 1981;1:297–311.

[10] Krohn KA, Link JM, Mason RP. Molecular imaging of hypoxia. J Nucl Med 2008;49(Suppl. 2):129S–48S.

[11] Mathews PM, Andermann F, Silver K, Karpati G, Arnold DL. Proton MR spectroscopic characterization of differences in regional brain metabolic abnormalities in mitochondrial encephalomyopathies. Neurology 1993;43:2484–90.

[12] Alger JR, Frank JA, Bizzi A, Fulham MJ, DeSouza BX, Duhaney MO, et al. Metabolism of human gliomas: assessment with H-1 MR spectroscopy and F-18 fluorodeoxyglucose PET. Radiology 1990;177:633–41.

[13] Gideon P, Henriksen O, Sperling B, Christiansen P, Olsen TS, Jorgensen HS, et al. Early time course of N-acetylaspartate, creatine and phosphocreatine, and compounds containing choline in the brain after acute stroke. A proton magnetic resonance spectroscopy study. Stroke 1992;23:1566–72.

[14] MunozManiega S, Cvoro V, Armitage PA, Marshall I, Bastin ME, Wardlaw JM. Choline and creatine are not reliable denominators for calculating metabolite ratios in acute ischemic stroke. Stroke 2008;39:2467–9.

[15] Aaen GS, Holshouser BA, Sheridan C, Colbert C, McKenney M, Kido D, et al. Magnetic resonance spectroscopy predicts outcomes for children with nonaccidental trauma. Pediatrics 2010;125:295–303.

[16] Ishii C, Oda A, Noda M, Taki M, Miyazawa T, Murase M, et al. Serum neuron-specific enolase in acute encephalopathy with febrile convulsive status epilepsticus (in Japanese). Shonika Rinsho (Tokyo) 2007;60:1702–6.

[17] Ishikawa J, Yamamuro M, Togawa M, Shiomi M. Attempt of differentiation acute encephalopathy with febrile convulsive status epilepticus from febrile convulsive status epilepticus induced by human herpesvirus 6 at early stage. No To Hattatsu 2010;42:283–6.

[18] Uemura O, Honda M, Matsuyama T, Ishikura K, Hataya H, Yata N, et al. Age, gender, and body length effects on reference serum creatinine levels determined by an enzymatic method in Japanese children: a multicenter study. Clin Exp Nephrol 2011;15:694–9.

[19] Waikar SS, Bonventre JV. Creatinine kinetics and the definition of acute kidney injury. J Am Soc Nephrol 2009;20:672–9.

[20] Andres RH, Ducray AD, Schlattner U, Wallimann T, Widmer HR. Functions and effects of creatine in the central nervous system. Brain Res Bull 2008;76:329–43.

[21] Marescau B, Deshmukh DR, Kockx M, Possemiers I, Qureshi IA, Wiechert P, et al. Guanidino compounds in serum, urine, liver, kidney, and brain of man and some ureotelic animals. Metabolism 1992;41:526–32.

[22] Tachikawa M, Kasai Y, Takahashi M, Fujinawa J, Kitaichi K, Terasaki T, et al. The blood–cerebrospinal fluid barrier is a major pathway of cerebral creatinine clearance: involvement of transporter-mediated process. J Neurochem 2008;107:432–42.
[23] Kubota M, Chida J, Hoshino H, Ozawa H, Koide A, Kashii H, et al. Thermolabile CPT II variants and low blood ATP levels are closely related to severity of acute encephalopathy in Japanese children. Brain Dev 2012;34:20–7.
[24] Ichiyama T, Suenaga N, Kajimoto M, Tohyama J, Isumi H, Kubota M, et al. Serum and CSF levels of cytokines in acute encephalopathy following prolonged febrile seizures. Brain Dev 2008;30:47–52.
[25] Nakagawa T, Fujita K, Saji Y, Maruyama A, Nagase H [Induced hypothermia/normothermia with general anesthesia prevents neurological damage in children with febrile refractory status epilepticus (in Japanese)]. No To Hattatsu 2011;43:459–63.
[26] Jacobs SE, Morley CJ, Inder TE, Stewart MJ, Smith KR, McNamara PJ, et al. Whole-body hypothermia for term and near-term newborns with hypoxic-ischemic encephalopathy: a randomized controlled trial. Arch Pediatr Adolesc Med 2011;165:692–700.
[27] Hypothermia after Cardiac Arrest Study G. Mild therapeutic hypothermia to improve the neurologic outcome after cardiac arrest. N Engl J Med 2002;346:549–56.
[28] Busto R, Globus MY, Dietrich WD, Martinez E, Valdes I, Ginsberg MD. Effect of mild hypothermia on ischemia-induced release of neurotransmitters and free fatty acids in rat brain. Stroke 1989;20:904–10.
[29] Iwata O, Iwata S, Thornton JS, De Vita E, Bainbridge A, Herbert L, et al. "Therapeutic time window" duration decreases with increasing severity of cerebral hypoxia-ischaemia under normothermia and delayed hypothermia in newborn piglets. Brain Res 2007;1154:173–80.

ELSEVIER

Brain & Development xxx (2015) xxx–xxx

BRAIN & DEVELOPMENT
Official Journal of the Japanese Society of Child Neurology

www.elsevier.com/locate/braindev

Case Report

Characteristic MRI features of chronic inflammatory demyelinating polyradiculoneuropathy

Yuichi Abe [a,*], Hiroshi Terashima [b], Hideki Hoshino [b], Kaori Sassa [a], Tetsuro Sakai [a], Akira Ohtake [a], Masaya Kubota [b], Hideo Yamanouchi [a]

[a] *Department of Pediatrics, Saitama Medical University, Saitama, Japan*
[b] *Division of Neurology, National Center for Child Health and Development, Tokyo, Japan*

Received 20 June 2014; received in revised form 28 January 2015; accepted 28 January 2015

Abstract

We present characteristic magnetic resonance imaging (MRI) features in a pediatric female patient with chronic inflammatory demyelinating polyradiculoneuropathy (CIDP). Muscle weakness developed at 8 years old and fluctuated during the clinical course over 7 years. Electrophysiological studies showed a demyelination pattern with moderately delayed nerve conduction velocity, as well as dispersion phenomenon. MRI showed marked changes in thickening of the spinal nerve roots and their peripheral nerves in the lumber and brachial plexuses, as well as in the bilateral trigeminal nerves. It is suggested that these MRI features are characteristic and strongly supportive of the diagnosis of CIDP with a prolonged clinical course.

Keywords: Chronic inflammatory demyelinating polyradiculoneuropathy; Peripheral nerve; Trigeminal nerve; Brachial plexus; Lumber plexus; Neurofibromatosis type 1; Hereditary motor and sensory neuropathy

1. Introduction

Chronic inflammatory demyelinating polyradiculoneuropathy (CIDP) is an acquired immune-mediated peripheral neuropathy which manifests with a progressive or relapsing nature over a period of 2 months [1]. Here, we present characteristic magnetic resonance imaging (MRI) features in a pediatric female patient with CIDP, whose clinical course stretched over 7 years. The striking and conclusive feature based on MRI identified in this case was marked changes in thickening, not only of the spinal roots and their peripheral nerves in the lumber and brachial plexuses, but also in the bilateral trigeminal nerves. It is suggested that these features are characteristic and strongly supportive of the diagnosis of CIDP with a prolonged clinical course.

2. Case report

This 15-year-old girl was referred to our hospital at 8 years of age because of resting pain in her proximal extremities and perioral region, as well as poor weight gain. Mild weakness developed soon after the first visit, and these symptoms remitted and became exacerbated repeatedly thereafter. She was born after 41 weeks of gestation and delivered normally. Her psychomotor development was normal. There was no family history of neuromuscular disorders, including polyneuropathy. Electrophysiological examination at 11 years of age showed low amplitudes of compound muscle action

* Corresponding author at: 38 Morohongo, Moroyama-machi, Iruma-gun, Saitama 350-0495, Japan. Tel./fax: +81 49 276 1219.
E-mail address: abeyped@saitama-med.ac.jp (Y. Abe).

http://dx.doi.org/10.1016/j.braindev.2015.01.006
0387-7604/

Please cite this article in press as: Abe Y et al. Characteristic MRI features of chronic inflammatory demyelinating polyradiculoneuropathy. Brain Dev (2015), http://dx.doi.org/10.1016/j.braindev.2015.01.006

potential (CMAP) and slow motor nerve conduction velocities (MCV) (Table 1) [2]. Although mild exacerbation and remission of symptoms reoccurred, she had been followed closely without any treatment.

At the age of 15 years, her neurological symptoms again relapsed. She ran very slowly and was unable to climb stairs or squat. Deep tendon reflexes were weak for the bilateral biceps and triceps brachii muscles and bilateral patellar reflexes were absent. She had no symptoms or signs associated with abnormalities of the trigeminal nerves or other cranial nerves. There was no skeletal deformation, in areas including the spine, foot and ankle joints. Grasping power was 5 kg in the left hand and 7 kg in the right. Muscle power of proximal upper and lower limbs was mildly reduced on manual muscle testing and graded at 3 to 4-/5. The modified Rankin score was grade 2. Decreased amplitudes of CMAP and abnormally slow MCV still remained in this period (Table 1). Blood biochemical examinations showed normal values. Autoimmune antibodies, including anti-nucleic acid antibody, and rheumatoid factor were negative. Anti-ganglioside antibodies, including anti-GM1, anti-GD1b and anti-GQ1b IgM class antibodies were all negative. A CSF study revealed a normal cell count at 1/μl and elevated protein at 243 mg/dl. The IgG index of CSF was 0.84. Myelin basic protein was lower than 40 pg/ml.

MRI (Fig. 1A–G) revealed marked changes in thickening of the spinal nerve roots and their peripheral nerves in the lumber and brachial plexuses, which were enhanced by gadolinium. These thickened nerves exhibited increased signal intensity on T2-weighted images, particularly evident on short tau inversion recovery (STIR) images. Brain MRI exhibited diffuse thickening of bilateral trigeminal nerves (arrowheads in Fig. 1H).

Table 1
Time series data of nerve conduction velocity.

	CMAP-Amp (mV)	MCV (m/s)	Temporal dispersion
11 years old			
Median N (R)	2.99/2.82 (W/E)	36.7	–
Ulnar N (R)	2.92/2.39 (W/below E)	**27.8**	–
Tibial N (R)	1.59/1.15 (A/P)	**20.8**	+
15 years old			
Median N (R)	0.78/1.14 (W/E)	**34.4**	–
Median N (L)	1.46/0.81 (W/E)	**31.3**	–
Ulnar N (R)	2.26/1.99 (W/below E)	37.6	+
Ulnar N (L)	2.08/1.67 (W/below E)	42.9	–
Tibial N (R)	2.01/1.08 (A/P)	**29.0**	+
Tibial N (L)	2.73/**1.24** (A/P)	32.2	+

CMAP: compound muscle action potential; Amp: amplitude; MCV: motor nerve conduction velocity; N: nerve; R: right; L: left; W: wrist; E: elbow; A: ankle; P: popliteal. Numbers in bold and underlined refer to a definitive diagnosis of CIDP based on the electrodiagnostic criteria [1], as follows: distal latency > 50% above upper limit of normal values [2]; <50% amplitude reduction of proximal negative peak of CMAP relative to distal and CMAP < 20% below lower limit of normal values [2]; MCV < 70% below lower limit of normal values [2].

Fluorescence *in situ* hybridization (FISH) analysis for duplication of the *PMP22* gene and microarray analysis for screening of 37 types of Charcot-Marie-Tooth disease (CMT) were negative. However, whole-exome sequencing demonstrated a heterozygous missense mutation in the *DYNC1H1* gene; c.370G>A, p. Val124-Met. We judged that this mutation was unlikely to play a causal role in her clinical manifestation, because the same mutation was found in her father, who had no symptoms or signs of polyneuropathy. The patient had clinical exacerbation 4 times over the following two years, during which time intravenous immunoglobulin therapies, as well as corticosteroid therapy, were administrated which were comparatively effective for the temporal remission of the symptoms.

3. Discussion

Thickening in the spinal nerve roots and their peripheral nerves in the lumbar and brachial plexuses has been reported as one of the characteristic features of CIDP in adult series with a prolonged clinical course [3]. The thickening of the peripheral nerves was found also in more distal parts, such as the sciatic nerve in this patient. In spite of these marked changes in thickening of the peripheral nerves, clinical manifestations were relatively mild. We suggest that a long clinical course with exacerbation and remission played a role in the appearance of these characteristic changes. Although widely distributed thickening of the peripheral nerves is also expected in neurofibromatosis type 1, as well as hereditary motor and sensory neuropathies (HMSN) such as CMT and Dejerine-Sottas disease [4], these changes are considered to be supportive of the diagnosis of CIDP.

In addition, markedly thickened bilateral trigeminal nerves were exhibited on MRI. Cranial nerve thickening in CIDP has been reported in adult series, as well as rarely in children [5–8]. Khadilkar showed hypertrophic trigeminal nerves in a 17-year-old female patient with CIDP, referred to as a "moustache sign" [6]. Costello reported a 17-year-old male patient with initial manifestations of childhood-onset CIDP, of chronic diplopia and generalized motor weakness, and MRI revealed thickening and enhancement of multiple cranial nerves, including oculomotor nerves [7]. Although thickening changes in the cranial nerves has been reported in the limited number of HSMN [9,10], these features are suggested as additional supportive MRI findings for the diagnosis of CIDP.

In conclusion, the characteristic MRI features found in this patient are strongly supportive findings for the diagnosis of CIDP, although several other neuropathic conditions may exhibit similar features. In addition to the MRI study, careful observations should be made based on a number of different studies, including investigation of clinical course and familial history,

Please cite this article in press as: Abe Y et al. Characteristic MRI features of chronic inflammatory demyelinating polyradiculoneuropathy. Brain Dev (2015), http://dx.doi.org/10.1016/j.braindev.2015.01.006

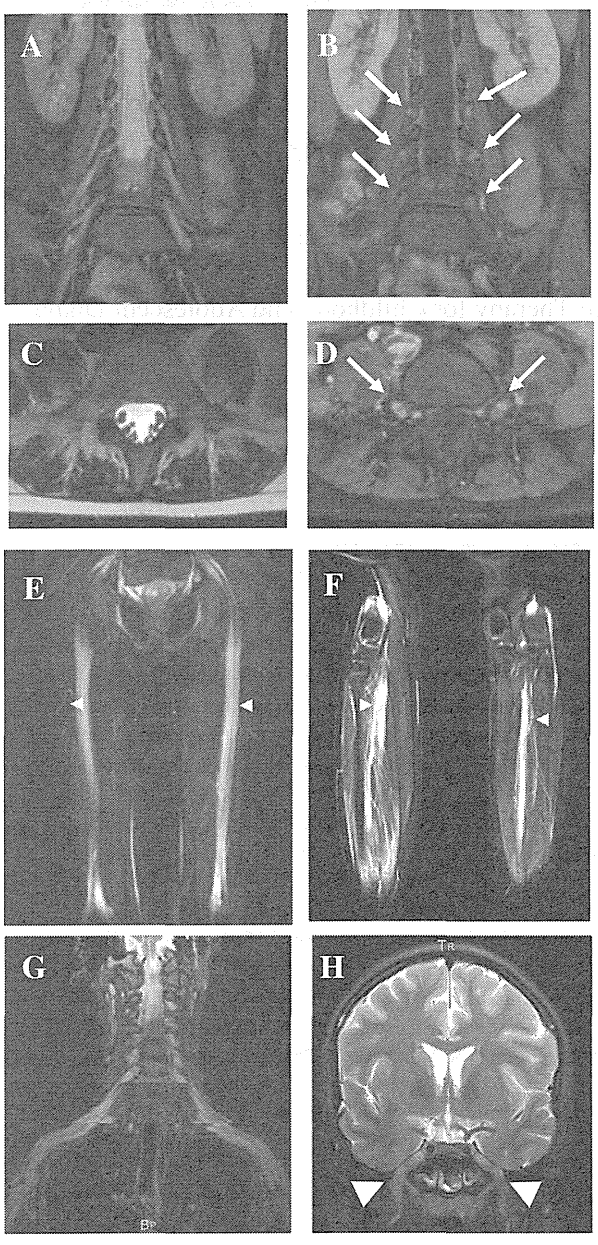

Fig. 1. MRI: T2-weighted image with short tau inversion recovery (T2W-STIR) (A, C and E–G); T1-weighted spin echo images with gadolinium-enhancement (B and D); and T2-weighted spin echo image (H). (A and B) are coronal images of the lumber and sacral levels. (C and D) are axial images of L5-S1 level. (E) and (F) are coronal images of the thighs and the lower legs, respectively. The spinal nerve roots and their peripheral nerves in the lumbar (A, B, C and D) and brachial plexuses (G) show changes in thickening and were enhanced with gadolinium (arrows in B and D). Ischiatic nerves and tibial nerves were markedly thickened (arrowheads in E and F, respectively). These thickened nerves exhibited high intensity on T2W-STIR images. The bilateral trigeminal nerves showed changes in thickening on coronal section (arrowheads in H). Each sequence is as follows: (A): TR/TE = 6000/64; (B): TR/TE = 500/10; (C): TR/TE = 4000/150; (D) TR/TE = 703/12; (E): TR/TE = 6450/65; (F): TR/TE = 4000/61; (G): TR/TE = 4210/42; and (H): TR/TE = 3500/150.

electrophysiological examinations, genetic analysis to exclude HMSN or other genetic neuropathic disorders, other autoimmune pathogenetic analysis, and responsiveness to immunotherapy, in order to define the diagnosis of CIDP.

Acknowledgements

We thank Dr. Hashiguchi and Dr. Takashima for genetic analysis of the patient and her parents. All genetic studies were performed upon receiving informed consent from the patient's parents, who indicated their approval through a document stating that the research will be conducted following the ethical guidelines for human genomic and genetic studies by the Ministry of Health, Labour and Welfare.

References

[1] Joint Task Force of the EFNS and the PNS. European Federation of Neurological Societies/Peripheral Nerve Society Guideline on management of chronic inflammatory demyelinating polyradiculoneuropathy: report of a joint task force of the European Federation of Neurological Societies and the Peripheral Nerve Society-First Revision. J Peripher Nerv Syst 2010;15:1–9.

[2] Cai F, Zhang J. Study of nerve conduction and late responses in normal Chinese infants, children, and adults. J Child Neurol 1997;12:13–8.

[3] Duggins AJ, McLeod JG, Pollard JD, Davies L, Yang F, Thompson EO, et al. Spinal root and plexus hypertrophy in chronic inflammatory demyelinating polyneuropathy. Brain 1999;122(Pt 7):1383–90.

[4] De Smet K, De Maeseneer M, Talebian Yazdi A, Stadnik T, De Mey J. MRI in hypertrophic mono- and polyneuropathies. Clin Radiol 2013;68:317–22.

[5] Niino M, Tsuji S, Tashiro K. Chronic inflammatory demyelinating polyneuropathy with multiple hypertrophic nerves in intracranial, and intra- and extra-spinal segments. Intern Med 1999;38:445–9.

[6] Khadilkar SV, Visana DR, Huchche AM, Shah N, Gupta N, Bharucha NE. Hypertrophic trigeminal nerves: moustache sign. Neurol India 2013;61:566–7.

[7] Costello F, Lee AG, Afifi AK, Kelkar P, Kardon RH, White M. Childhood-onset chronic inflammatory demyelinating polyradiculoneuropathy with cranial nerve involvement. J Child Neurol 2002;17:819–23.

[8] Guibord N, Chalk C, Wein F, Richardson J, Snipes GJ, Del Carpio R. Trigeminal nerve hypertrophy in chronic inflammatory demyelinating polyradiculoneuropathy. Neurology 1998;51:1459–62.

[9] Yener GG, Guiochon-Mantel A, Obuz F, Baklan B, Ozturk V, Kovanlikaya I, et al. Phe 84 deletion of the PMP22 gene associated with hereditary motor and sensory neuropathy HMSN III with multiple cranial neuropathy: clinical, neurophysiological and magnetic resonance imaging findings. J Neurol 2001;248:193–6.

[10] Aho TR, Wallace RC, Pitt AM, Sivakumar K. Charcot-Marie-Tooth disease: extensive cranial nerve involvement on CT and MR imaging. Am J Neuroradiol 2004;25:494–7.

Please cite this article in press as: Abe Y et al. Characteristic MRI features of chronic inflammatory demyelinating polyradiculoneuropathy. Brain Dev (2015), http://dx.doi.org/10.1016/j.braindev.2015.01.006

ORIGINAL

Advance Publication
doi: 10.1507/endocrj. EJ14-0066

The ratio of glycated albumin to hemoglobin A1c measured in IFCC units accurately represents the glycation gap

Junya Akatsuka[1], Mie Mochizuki[2], Ikuma Musha[1], Akira Ohtake[1], Kisho Kobayashi[2], Toru Kikuchi[3], Nobuyuki Kikuchi[4], Tomoyuki Kawamura[5], Tatsuhiko Urakami[6], Shigetaka Sugihara[7], Tadao Hoshino[8] and Shin Amemiya[1], the Japanese Study Group of Insulin Therapy for Childhood and Adolescent Diabetes

[1] *Department of Pediatrics, Saitama Medial University, Saitama 350-0495, Japan*
[2] *Department of Pediatrics, University of Yamanashi, Yamanashi 409-3898, Japan*
[3] *Division of Pediatrics, Department of Homeostatic Regulation and Development, Niigata University Graduate School of Medical and Dental Sciences, Niigata 950-2181, Japan*
[4] *Department of Pediatrics, Yokohama City University Medical Center, Kanagawa 232-0024, Japan*
[5] *Department of Pediatrics, Osaka City University Graduate School of Medicine, Osaka 545-8585, Japan*
[6] *Department of Pediatrics and Child Health, Nihon University School of Medicine, Tokyo 173-8610, Japan*
[7] *Department of Pediatrics, Tokyo Women's Medical University Medical Center East, Tokyo 119-8567, Japan*
[8] *Institute of Biopathological Medicine, Kanagawa 243-0813, Japan*

Abstract. The glycation gap (G-gap: difference between measured hemoglobin A1c [A1C] and the value predicted by its regression on the fructosamine level) is stable and associated with diabetic complications. Measuring A1C level in International Federation of Clinical Chemistry (IFCC) units (A1C-SI; mmol/mol) and National Glycohemoglobin Standardization Program units (A1C-NGSP; %) and using glycated albumin (GA) level instead of fructosamine level for calculating the G-gap, we investigated whether the G-gap is better represented by GA/A1C ratio if expressed in SI units (GA/A1C-SI ratio) rather than in NGSP units (GA/A1C-% ratio). We examined 749 Japanese children with type 1 diabetes using simultaneous GA and A1C measurements. Of these, 369 patients were examined more than five times to assess the consistency of the G-gap and the GA/A1C ratio within individuals. The relationship of GA/A1C-% ratio to the corresponding A1C-NGSP was stronger than that of GA/A1C-SI ratio to A1C-IFCC. At enrollment, the inverse relationship between the GA/A1C-SI ratio and G-gap was highly significant ($R^2 = 0.95$) compared with that between the GA/A1C-% ratio and G-gap ($R^2 = 0.69$). A highly significant inverse relationship was also observed between the mean GA/A1C-SI ratio and the mean G-gaps obtained individually over time ($R^2 = 0.95$) compared with that using the corresponding A1C-NGSP ($R^2 = 0.67$). We conclude that the G-gap is better represented by the GA/A1C-SI ratio. We propose the use of mean GA/A1C-SI ratios easily obtained individually over time as reference values in Japanese children with type 1 diabetes (6.75 ± 0.60 [means ± SD]).

Key words: Hemoglobin A1c, Glycated albumin, Type 1 diabetes mellitus, Glycation gap, SI units

THE ONSET and progression of diabetic complications are important issues in the long-term management of type 1 diabetes. In the Diabetes Control and Complications Trial (DCCT), poor glycemic control shown by a high HbA1c (A1C) value was reported to be an important risk factor [1, 2]. Inter-individual biological variation in A1C, which is distinct from that attributable to mean blood glucose, was also evident among type 1 diabetic patients in the DCCT and was a strong predictor of risk of diabetes complications [3, 4].

Cohen *et al.* [5] suggested that the excess inter-individual variation in A1C would be explained by a "glycosylation gap," the difference between the measured A1C concentration and that predicted by the fructosamine concentration. They also described a relationship between the glycation gap (G-gap) and diabetic complications. Nayak *et al.*, considering the biological variability of the G-gap, reported that it was an indica-

Submitted Feb. 13, 2014; Accepted Oct. 9, 2014 as EJ14-0066
Released online in J-STAGE as advance publication Oct. 31, 2014
Correspondence to: Shin Amemiya, Department of Pediatrics, Saitama Medical University, 38 Morohongo, Moroyama-machi, Iruma-gun, Saitama 350-0495, Japan.
E-mail: shin_a@saitama-med.ac.jp
*Junya Akatsuka and Mie Mochizuki contributed equally as the first authors. The rest of co-authors are listed following acknowledgement.

tor that showed consistency over the long term for individuals [6]. Rodriguez-Segada *et al.* reported that the G-gap was a non-glycemic determinant that was a risk factor independent of A1C for the progression of complications [7]. However, Sacks *et al.* noted that this assertion was not necessarily supported [8].

The expression of A1C values in both National Glycohemoglobin Standardization Program (NGSP) units (A1C-NGSP) and International Federation of Clinical Chemistry (IFCC) units (A1C-IFCC) has been accepted for the global harmonization of the A1C standardization in main international diabetes journals and meetings. This harmonization is accomplished using conversion formulas for A1C-NGSP and A1C-IFCC [9]. These conversion formulas are not necessarily applied in regular medical practice in each country or region where either A1C-NGSP or A1C-IFCC has been used to assess the degree of glycemic control [10].

Although the relationship between A1C-NGSP values and A1C-IFCC values is described by a straight line, the slope of the line differs significantly from 1 and its intercept differs from 0 [10]. A phenomenon similar to that experienced with the NGSP system is observed in the relationships between A1C-IFCC values and A1C values obtained by the other designated comparison methods in Japan and Sweden [11]. We accordingly focused on how the GA/A1C ratio might be affected by the corresponding A1C values themselves in A1C-IFCC and A1C-NGSP units, owing to differences in the underlying measurement systems. The A1C value obtained with each designated comparison method, including the conventional A1C-NGSP value, incorporates interfering factors such as non-glycated hemoglobins, but A1C-IFCC does not theoretically incorporate non-glycated hemoglobin [12, 13]. It should thus be noted that the effect of A1C-IFCC and A1C-NGSP units on proportional evaluation in relation to other glycemic indexes such as GA or fructosamine may result in some differences in the G-gap and the GA/A1C ratio obtained in the respective units.

In the present study, we compared the G-gap between simultaneously measured A1C and glycated albumin (GA). We used GA, a glycated product of albumin, instead of fructosamine to measure glycated proteins in serum (of which glycated albumin is the main component) [14, 15]. Although the GA assay has not yet been approved by the Food and Drug Administration (FDA) and may not be available in the United States of America, Nathan *et al.* reported that independently of A1C, GA was associated with diabetic complications in the DCCT/Epidemiology of Diabetes Interventions and Complications (EDIC) study [16]. Furthermore, Selvin *et al.* reported the prediction of incident diabetes and microvascular complications by both fructosamine and GA [17]. The prediction power differed little between fructosamine and GA. The G-gap has been obtained using data for simultaneously measured fructosamine and A1C in a given specific population, and thus, is difficult to use as an indicator in regular medical practice. In contrast, the GA/A1C ratio is obtained from measurement results only. If reference values were established for the same race, age, disease, and disease type, the GA/A1C ratio could be used as an indicator representing the G-gap in regular medical practice.

An individual's GA value reflects glycemic control in the preceding 2–4 weeks and changes over a shorter time than A1C. The GA/A1C ratio is thus affected by short-term blood glucose fluctuations [18]. The GA/A1C ratio is also reported to be affected by diabetes type [19-22], obesity [23, 24], and other factors such as a short time after the initial treatment of diabetes [20, 22-24]. GA can be affected by liver and kidney diseases disturbing albumin metabolism and A1C can be affected by hemoglobinopathy, anemia, and other disorders [16]. In contrast, an important aspect of the G-gap is that it can be treated as an intrinsic value that is consistent for each individual over time as a predictor of diabetic complications independent of A1C [6].

Rodriguez-Segada *et al.* suggested the need to obtain a G-gap specific to the individual under relatively stable glycemic control in order to avoid the effects of short-term blood glucose fluctuations [25]. In the present study, individual intrinsic GA/A1C ratios were obtained as means of multiple measurements, and we investigated whether the GA/A1C ratio could be used in place of the G-gap.

Materials and Methods

Subjects

The subjects included type 1 diabetes patients with childhood onset at the age of <16 years, enrolled in the third cohort as of March 1, 2008, of a multicenter study by the Japanese Study Group of Insulin Therapy for Childhood and Adolescent Diabetes. The subjects were <18 years of age at the time of registry (as on December 31st, 2007). This observational study was

approved by each participating institution's review board, and written consent was obtained from the patients/siblings or their parents. The study was conducted by the 58 institutes listed as coauthors.

Group A consisted of 749 patients whose GA and A1C values were measured simultaneously at enrollment and for whom information including gender, age, duration of disease, insulin dose, height, and weight was obtained. Body mass index (BMI) was calculated from body height and weight. The BMI standard deviation score (SDS) was also obtained by age and gender for the Japanese population [26]. Patients whose duration of disease was less than 6 months were excluded because of the possibility that the GA/A1C ratio would vary greatly owing to rapid improvements in glycemic control. No patients showed disorders affecting albumin metabolism and hemoglobinopathy.

Group B consisted of 369 patients from Group A whose GA and A1C were measured simultaneously five times or more over observation periods every 4 months in the subsequent 3 years.

Group C consisted of 62 non-diabetic siblings of a group A patient whose GA and A1C were measured simultaneously at enrollment in the third cohort of this Study Group.

In this study, many patients in type 1 diabetes mellitus used carbohydrate counting and changed insulin dose in each meal. Thus, blood glucose excursion and insulin dose was estimated to be not stable.

The profiles of groups A, B, and C are shown in Table 1.

Biochemical analyses

The A1C and GA values of patients at enrollment were measured by the same general test organization (SRL Inc., Tokyo, Japan), and reproducibility of A1C values was confirmed with the Japan Diabetes Society (JDS) calibrator. A1C was measured by automated HPLC analysis (HLC-723G8, Tosoh Corp., Tokyo), and GA was determined by an enzymatic method using a liquid chemistry system (Lucica GA-L method, Asahi Kasei Corp., Tokyo) [27, 28].

In the subsequent observation periods, measurement data at each institution were used for GA and A1C. To control accuracy, the GA-% and A1C-JDS values for four patients at each center were also measured by the general test organization, and we investigated the relative error between the measurement values obtained by the general test organization and the measurement values obtained at each institution. The mean relative errors for the A1C-JDS value and GA-% were 2.4% and 2.8%, respectively, and the difference between par-

Table 1 Characteristics and data of type 1 diabetes patients and their non-diabetic siblings

	Group A (n = 749) Type 1 diabetes at enrollment (1st period)	**Group B (n = 369)** Type 1 diabetes with data obtained > 5 times	**Group C (n = 62)** Non-diabetic siblings
Age (years)	12.1 ± 3.9 (12.6: 9.5–15.2)	12.1 ± 3.8 (12.3: 9.2–15.1) §	12.3 ± 5.5 (13.0: 8.0–16.0)
Duration (years)	7.0 ± 3.8 (6.8: 3.6–10.1) †	5.2 ± 3.5 (4.3: 2.4–7.3) §	NA
BMI (kg/m^2)	19.7 ± 3.5 (19.4: 17.0–21.9)	19.5 ± 3.5 (19.2: 17.0–21.6) §	19.3 ± 3.7 (18.5: 17.0–20.6)
Dose of insulin per weight (U/weight)	1.07 ± 0.34 (1.04: 0.85–1.27) †	1.12 ± 0.33 (1.08: 0.88–1.30)	NA
A1C-NGSP (%)	7.8 ± 1.1 (7.7: 7.1–8.5) †‡	8.0 ± 1.0 (7.9: 7.3–8.6) ‡	5.2 ± 0.2 (5.1: 5.0–5.4)
A1C-IFCC (mmol/mol)	62.0 ± 12.6 (60.6: 53.9–69.5) †‡	63.6 ± 10.8 (62.8: 55.7–70.6) ‡	33.2 ± 2.5 (32.7: 31.6–35.0)
GA-% (%)	23.8 ± 4.9 (23.1: 20.5–26.5) ‡	23.7 ± 4.0 (23.5: 20.8–26.1) ‡	13.6 ± 1.0 (13.7: 12.9–14.2)
GA-SI (mmol/mol)	430.4 ± 93.3 (416.7: 367.0–481.7) ‡	427.9 ± 77.3 (424.4: 371.8–473.9) ‡	235.6 ± 19.1 (236.0: 221.2–247.1)
GA/A1C-%	3.03 ± 0.30 (3.02: 2.82–3.23) †‡	2.96 ± 0.25 (2.95: 2.77–3.15) ‡	2.63 ± 0.21 (2.65: 2.49–2.77)
GA/A1C-SI	6.95 ± 0.70 (6.94: 6.49–7.42) †	6.75 ± 0.60 (6.73:6.31–7.17)‡	7.13 ± 0.72 (7.11: 6.71–7.61)
Mean CV (%) of GA/A1C-%	NA	6.95 ± 2.91 (6.46: 5.02–8.23)	NA
Mean CV (%) of GA/A1C-SI	NA	7.23 ± 3.23 (6.70: 5.04–8.62)	NA

§: the data at enrollment; other data in group B were obtained by the mean value in each patient with data obtained more than 5 times over 3 years. Data are means ± SD, (median; interquartile range). CV, coefficient of variation; NA, not applicable. *p* value; †:<0.05 vs. group B, ‡:<0.05 vs. group C.

ticipating institutions was judged acceptable.

The A1C value was first expressed uniformly as the NGSP value using conversion formula for the JDS and NGSP values that were rated with respect to JDS calibrator lot 4 (A1C-NGSP value (%) = 1.02 × A1C-JDS value (%) + 0.25) [29]. The A1C- IFCC value was also obtained from the A1C-NGSP value using the conversion formula (A1C-IFCC value (mmol/mol) = 10.93 × A1C-NGSP value (%) − 23.52) [9].

In expressing the GA value, the GA-% value measured by Lucica GA-L was converted to SI values (GA-SI) in accordance with a committee report of the Japan Society of Clinical Chemistry (GA-SI (mmol/mol) = {GA-% − 1.306}/0.0523) [30]). The GA/A1C ratio was expressed by GA/A1C-SI when the SI value was used and by GA/A1C-% when the conventional % value was used.

For the G-gap, following the reports of Macdonald *et al.* [31] and Nayak *et al.* [6], fructosamine was replaced with GA, and GA-derived A1C = {[(GA−GA(M))/GA(SD)] × A1C (SD)} + A1C (M) was obtained. The G-gap was then obtained as G-gap = the HbA1c measured value − the GA-derived A1C (M and SD indicate mean and standard deviation, respectively).

Consistency of the G-gap within individuals over time

To test the hypothesis that the G-gap is consistent in direction within individuals over time, a quadratic curve was plotted as the product of any G-gap pair in two different periods (as the y-axis) against the G-gap at a certain period (as the x-axis). If any G-gap pair in two different periods were concordant, the product would be positive (i.e., above the x-axis: positive × positive = positive, negative × negative = positive) in a quadratic curve that passed through the origin. If any pairs showed discordance, the product would be negative (below the x-axis: negative × positive = negative). The correlation coefficients were obtained in quadratic curves calculated over time.

Effect of A1C expressed by either IFCC units or NGSP units on the GA/A1C ratio and G-gap

The GA/A1C ratio correlated positively with A1C-NGSP and negatively with A1C-IFCC in the present study, indicating that the GA/A1C ratio might be affected by either A1C-NGSP or A1C-IFCC levels in relation to the G-gap. We accordingly used the adjusted GA/A1C-% ratio and the adjusted GA/A1C-SI ratio for the evaluation of the relationship with the G-gap in place of those using the raw GA/A1C-% ratio and the raw GA/A1C-SI ratio, respectively. To eliminate the effects of A1C-NGSP and A1C-IFCC on the GA/A1C-% and GA/A1C-SI ratios, respectively, a slope in the linear relationship between GA/A1C ratios and the corresponding A1C values was made flat. An adjusted GA/A1C-% ratio was obtained for each individual by subtracting the increased portion in the GA/A1C-% ratio value (ΔGA/A1C-% ratio) from a defined A1C-NGSP value to the corresponding raw A1C-NGSP value. In this study, A1C-NGSP values of 5.2, 5.7, 6.5, and 9% were assigned as non-diabetic, impaired glucose intolerant, diabetes diagnostic, and poor glycemic-control values, respectively. An adjusted GA/A1C-% ratio was calculated as (raw GA/A1C-% ratio − ΔGA/A1C-% ratio), where ΔGA/A1C-% ratio = the slope (in the correlation between the raw GA/A1C-% ratios and the corresponding A1C-NGSP values) * ΔA1C-NGSP (between the corresponding raw A1C-NGSP value and four selected A1C-NGSP values of 5.2, 5.7, 6.5 and 9%). The same calculation was also applied for the adjusted GA/A1C-SI ratios.

Suitability of GA/A1C-ratio for representing the G-gap

The correlation between G-gap and GA/A1C-ratio was calculated for each period, as was the correlation between the respective mean values using either A1C-NGSP or A1C-SI. Correlations were also calculated for the adjusted GA/A1C-% and GA/A1C-SI ratios.

Statistical analyses

Comparisons of GA/A1C ratios between groups A, B, and C were made with the Mann–Whitney test. Factors affecting the GA/1A1C ratio at enrollment in group A were evaluated by stepwise analysis with the GA/A1C ratio as the response variable and gender, age, duration of disease, insulin dose, BMI-SDS, and A1C-NGSP or A1C-SI as explanatory variables. The normality of the distributions of the GA/A1C ratio and G-gap was evaluated with the Shapiro–Wilk test.

All statistical analyses were performed using JMP (version 8.0; SAS Institute Inc., Cary, NC, USA). Descriptive statistical analyses were performed with SAS statistical software (version 9.3; SAS Institute Inc., Cary, NC, USA). A probability level of <0.05 was considered significant.

Results

Comparison of the GA/A1C ratio in type 1 diabetes patients (group A) and their siblings

No significant differences in age and BMI were revealed between the diabetic patients and their siblings. However, A1C-NGSP, A1C-SI, GA-%, and GA-SI were all significantly higher in the type 1 diabetes patients. Of the GA/A1C ratios, the GA/A1C-% ratio was significantly higher in group A, whereas the GA/A1C-SI ratio was significantly lower in the diabetic patients than in their siblings (Table 1).

The GA/A1C ratio at enrollment and related factors

The GA/A1C-% ratio was positively correlated with A1C-NGSP: (GA/A1C-% ratio = 0.086A1C-NGSP + 2.356 , $R^2 = 0.105$, $p < 0.0001$), and the step-wise analysis with the GA/A1C-% ratio showed positive correlations with A1C-NGSP and age (years), and negative correlations with BMI-SDS, dose of insulin per weight (units/kg), and duration (years): GA/A1C-% ratio = 2.274 + 0.088 (A1C-NGSP) + 0.023 (age) − 0.051 (BMI-SDS) + 0.112 (dose of insulin per weight) − 0.011 (duration) (R^2= 0.181). In contrast, the GA/A1C-SI ratio was negatively correlated with A1C-IFCC: (GA/A1C-SI = −0.007A1C-IFCC+7.358, R^2 = 0.014, p = 0.001) and the stepwise analysis with the GA/A1C-SI ratio showed a weak positive correlation with age and negative correlations with BMI-SDS, A1C-SI, dose of insulin per weight, and duration: GA / A1C-SI ratio = 7.149 + 0.055 (age) − 0.118 (BMI-SDS) − 0.300 (dose of insulin per weight) − 0.006 (A1C-SI) − 0.021 (duration) (R^2 = 0.093).

Consistency of the G-gap within individuals over time

When the G-gap in 1st, 4th, and 7th periods of the 1st and 4th, 4th and 7th, and 7th and 10th periods of approximately 1 year each and that in 1st periods of the 1st and 10th periods of approximately 3 years were plotted on the x-axis for group B, and the product of individual G-gap pairs in two periods was plotted on the y-axis, a quadratic curve that passed through the origin was obtained for the G-gap with GA and A1C (Fig. 1). The multiple correlation coefficients R^2 for the G-gap and the product of G-gap pairs in two different periods were 0.28 to 0.51, as shown in Table 2 A and Fig.1 A-1 and A-2. The correlation coefficients were significantly higher when the mean G-gap values were used (Fig. 1 B-1 and B-2). There was no difference between the G-gap based on A1C-IFCC and that based on A1C-NGSP.

Effect of A1C expressed by either IFCC units or NGSP units on the GA/A1C ratio and G-gap

The G-gap and the GA/A1C ratio both showed significant negative correlations, but a stronger correlation was shown when the A1C-IFCC value was used: G-gap-% = −1.52 GA/A1C-% ratio + 4.61, R^2 = 0.69, $p < 0.0001$ vs. G-gap-SI = −8.46 GA-/A1C-SI ratio + 58.81, R^2 = 0.95, $p < 0.0001$, at the first period of enrollment, n = 749 of group A (Table 3, Fig. 2 group A 1-a and 2-a).

The multiple correlation coefficients for the GA/A1C-SI ratio and the G-gap-SI in each period were higher than those for the GA/A1C-% ratio and the G-gap-%, as shown in Table 3. Given that the GA/A1C-% ratio showed a positive correlation with A1C-NGSP (ex. GA/A1C-% ratio = 0.088 A1C-NGSP + 2.35, $R^2 = 0.105$, $p < 0.0001$, in the first period of group B, n = 369), we adjusted the raw GA/A1C-% ratio by the subtraction of the ΔGA/A1C-% ratio between four selected A1C-NGSP values (5.2, 5.7, 6.5 and 9.0%) and the corresponding A1C-NGSP values as shown in Table 3 (left side). Likewise, adjusted GA/A1C-SI ratios were calculated at 33, 39, 48, and 75 mmol/mol of A1C-IFCC (right side).

The effect of adjustment by A1C-NGSP values from 5.2% to 6.5% on the correlation coefficient with G-gap showed almost the same improvement. The correlation between the adjusted GA/A1C-% ratio and G-gap-% was repeatedly improved compared to that between the corresponding raw GA/A1C-% ratio and G-gap-% in each subsequent period (Table 3 left side, Fig. 2 left side panels). The improvement after adjustment was less noted at 9.0% of A1C-NGSP.

In contrast, no significant change or improvement was observed when the same calculation was applied for the adjusted GA/A1C-SI ratio (Table 3 right side, Fig. 2 right side panels).

The mean values (± SD) and medians (interquartile range) from several measurements of the GA/A1C ratio and G-gap for each patient are shown in Table 1. The mean GA/A1C ratio and the mean G-gap both exhibited normal distributions. There was a significant negative correlation between the mean GA/A1C ratio and the mean G-gap. For the raw GA/A1C-SI ratio in particular, a high correlation with the mean G-gap (R^2 of 95%) was obtained (Table 3, Fig. 2 group B 2-a).

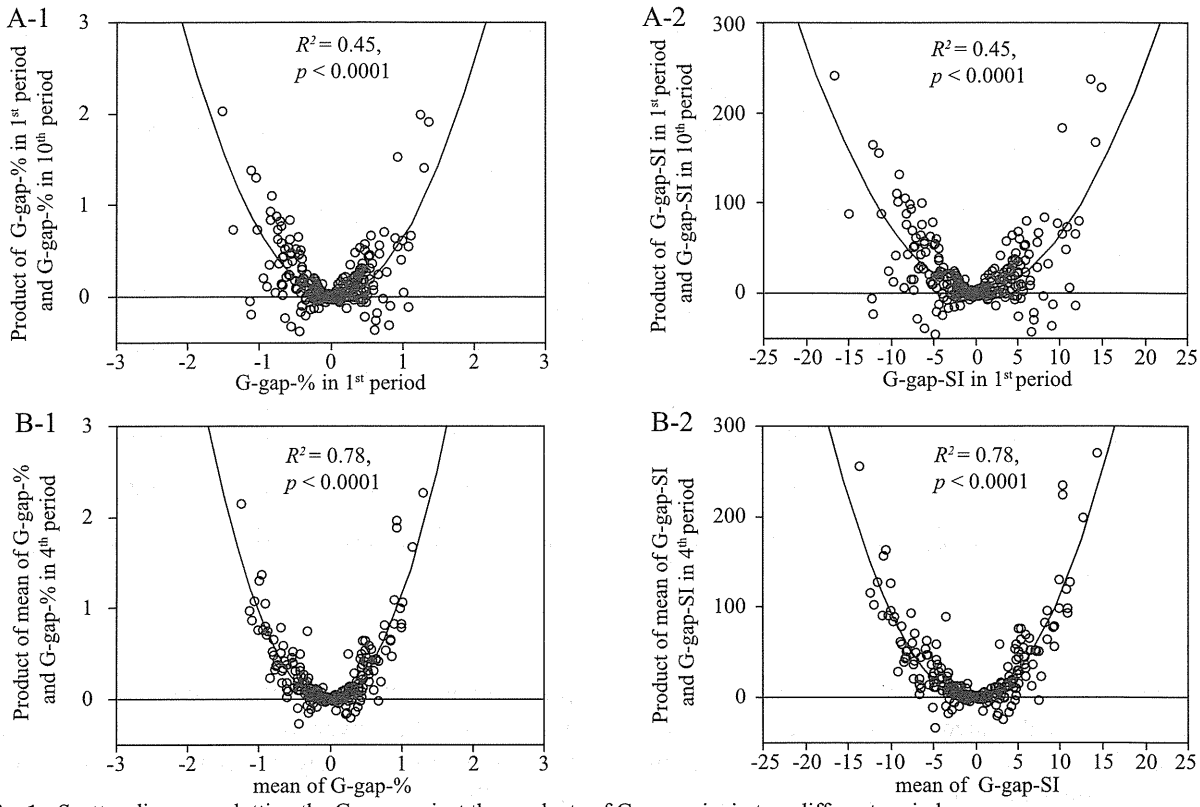

Fig. 1 Scatter diagrams plotting the G-gap against the products of G-gap pairs in two different periods.
A: The G-gap in the first period on the x-axis and products of G-gap pairs in the first and tenth periods on the y-axis (n = 242).
B: The mean G-gap individually obtained more than 5 times on the x-axis against the products of the mean G-gap and G-gap in the fourth period on y-axis (n = 229). A-1 and B-1: based on G-gap-%; A-2 and B-2: based on G-gap–SI. The correlation coefficients were significantly higher when mean G-gap values (B-1 and B-2) were used, suggesting that individual consistency of the G-gap may be obtained by mean values over time. See also Table 2.

Table 2
A: Correlation coefficients between products of G-gap pairs and G-gap individually obtained in two different periods

Periods	R^2 based on GA-% and A1C-NGSP	R^2 based on GA-SI and A1C-SI
1st vs. 4th (1 year apart) (n = 229)	0.45	0.45
4th vs. 7th (1 year apart) (n = 208)	0.28	0.28
7th vs. 10th (1 year apart) (n = 213)	0.51	0.51
1st vs. 10th (3 years apart) (n = 242)*	0.45	0.45

*see also Fig. 1, A-1 and A-2

B: Correlation coefficients between products of G-gap pairs using each period G-gap and the mean of G-gap and the latter

Periods	R^2 based on GA-% and A1C-NGSP	R^2 based on GA-SI and A1C-SI
1st (n = 369)	0.58	0.58
4th (n = 229) **	0.78	0.78
5th (n = 320)	0.78	0.78
6th (n = 342)	0.75	0.75
7th (n = 327)	0.76	0.76
8th (n = 353)	0.83	0.83
9th (n = 314)	0.81	0.81
10th (n = 242)	0.84	0.84

**see also Fig. 1 B-1 and B-2.

Table 3 Correlation coefficient between G-gap and GA/A1C ratio in each period using either A1C-NGSP or A1C-SI and those of the mean values

Periods	R^2 in case of A1C-NGSP					R^2 in case of A1C-IFCC				
	Raw values	after adjustment adjusted at A1C-NGSP(%) =				Raw values	after adjustment adjusted at A1C-IFCC (mmol/mol) =			
		5.2	5.7	6.5	9.0		33	39	48	75
1st (n = 369)	0.67	0.89	0.89	0.88	0.72	0.96	0.91	0.91	0.91	0.95
4th (n = 229)	0.75	0.93	0.93	0.92	0.8	0.95	0.92	0.92	0.92	0.94
5th (n = 320)	0.68	0.88	0.88	0.87	0.73	0.93	0.88	0.88	0.88	0.91
6th (n = 342)	0.7	0.9	0.9	0.89	0.76	0.94	0.89	0.89	0.89	0.93
7th (n = 327)	0.63	0.85	0.85	0.85	0.7	0.9	0.82	0.82	0.82	0.88
8th (n = 353)	0.74	0.91	0.91	0.91	0.78	0.94	0.9	0.9	0.9	0.93
9th (n = 314)	0.75	0.91	0.91	0.91	0.81	0.93	0.88	0.88	0.88	0.92
10th (n = 242)	0.72	0.91	0.91	0.9	0.77	0.95	0.89	0.89	0.89	0.93
Mean value in each patients (n = 369)	0.67	0.89	0.89	0.88	0.72	0.95	0.88	0.88	0.88	0.93

Adjustment was made by eliminating the effect of the slope on the correlation either between GA/A1C-% and A1C-NGSP or between GA/A1C-SI ratio and A1C-IFCC. See also Fig. 2

Although linear correlations between G-gaps and GA/A1C ratios were calculated by the total data of groups B and C, the correlation depicted a cluster of group C of the non-diabetic siblings separately from that of group B of type 1 diabetes children and adolescents (Fig. 2 groups B and C panels). The descriptive statistical analyses revealed that the GA/A1C ratios in group B were significantly different from those in group C.

Thus, in this investigation, the mean GA/A1C-SI ratios obtained individually over time were 6.75 ± 0.60 (6.73: 6.31–7.17) in Japanese pediatric type 1 diabetes patients highly correlated inversely with the G-gap (Table 1, Fig. 2 group B 2-a).

Discussion

In this study, we used GA instead of fructosamine for calculating the G-gap. GA is formed by the attachment of glucose to albumin. Fructosamine is formed by the covalent attachment of glucose to total serum proteins, primary albumin [14, 15]. GA is not affected by other glycated proteins in serum, compared with fructosamine which is including glycated proteins other than albumin. Selvin *et al.* reported the prediction of incident diabetes and microvascular complications by both fructosamine and GA [17]. Thus, GA is considered to be almost biologically equal to fructosamine for calculating G-gap.

We have demonstrated for the first time that the GA/A1C-SI ratio using A1C-IFCC showed more accurate representation of the G-gap than the GA/A1C-% ratio using A1C-NGSP, given that the mean GA/A1C-SI ratio was highly inversely correlated with the G-gap (Table 3, Fig. 2).

Concerning the strength of the GA/A1C-SI ratio in this study, the GA/A1C ratio can be determined with simultaneous measurements of GA and A1C and is thus generally used in regular clinical practice, whereas the G-gap has been obtained only in specific populations and is not suitable for use in other populations. In the present study, although the GA/A1C ratios could not be determined under conditions of stable glycemic control, the multiple correlation coefficients R^2 for the G-gap and the product of G-gap pairs in two different periods were 0.28 to 0.51, consistent with the values of 0.39 to 0.52 reported by Nayak *et al.* [6]. Furthermore, the correlation coefficients were significantly higher when mean G-gap values were used (Fig. 1 B-1 and B-2). The mean GA/A1C ratio individually obtained from multiple measurements was accordingly considered as the intrinsic value for each patient. There was a significant correlation between the mean GA/A1C ratio and the G-gap in each patient, especially the mean raw GA/A1C-SI ratio showing a very high correlation with the G-gap, R^2 of 95%. (Table 3 right, Fig. 2 group B right panels). GA/A1C-SI ratio between measurements showed a CV of 7% as an intrinsic value for most individuals (Table 1 group B).

In comparison to previous reports describing the G-gap and the GA/A1C ratio, our study has clarified

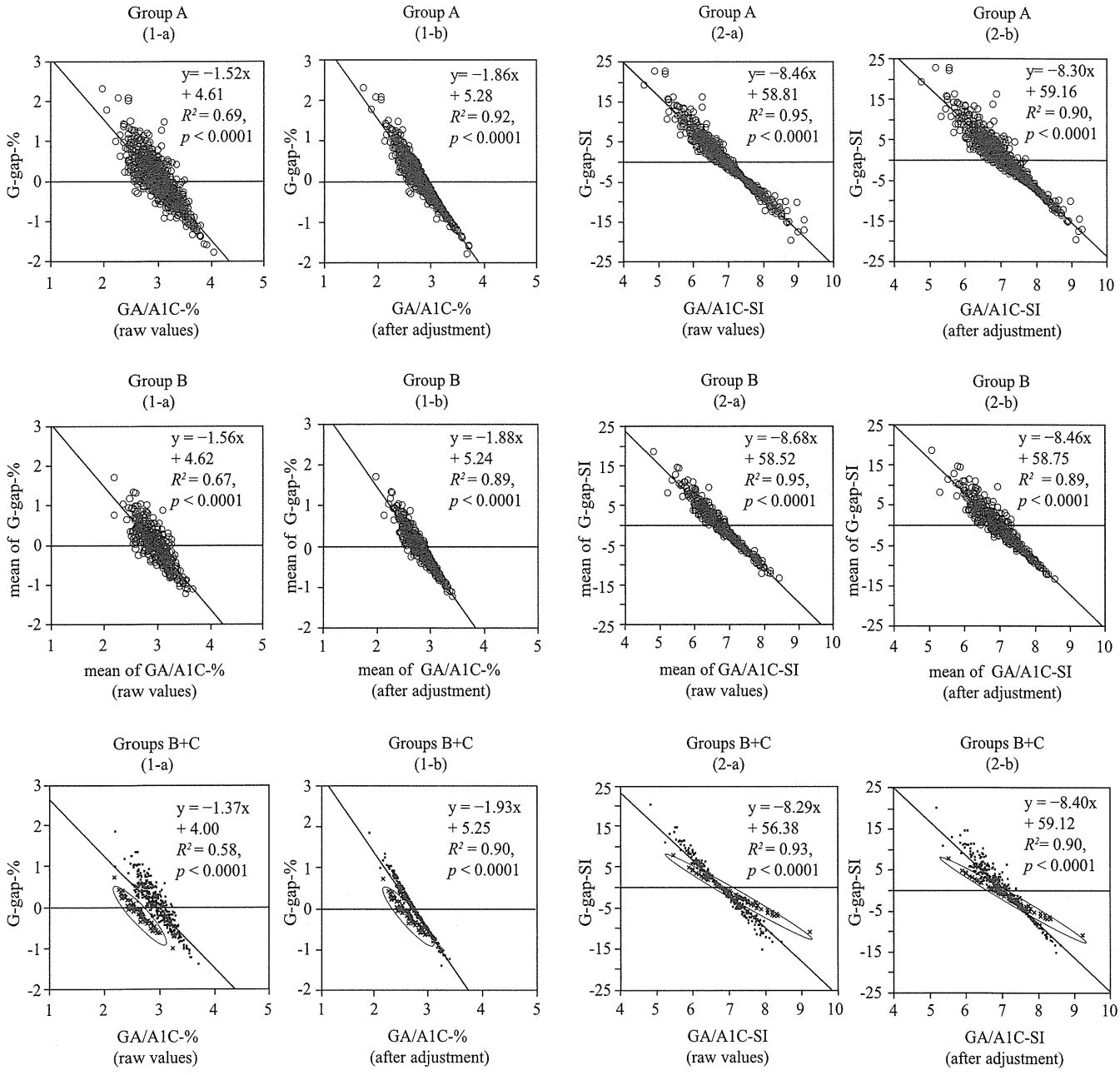

Fig. 2 Correlation between G-gap and GA/A1C ratio

A more accurate representation of the G-gap was obtained by GA/A1C-SI ratios (on the right side; 2-a by raw values and 2-b after adjustment) than by GA/A1C-% ratios (on the left side; 1-a by raw values and 1-b after adjustment).

The adjustment was made at A1C-NGSP = 5.7% for GA/A1C-% or at A1C-SI = 39 mmol/mol for GA/A1C-SI ratios. Significant improvement of the correlation coefficients after the adjustment was shown in case of the GA/A1C-% ratios, whereas the use of GA/A1C-SI ratios showed higher correlation without the adjustment. (See also Table 3)

The top four panels show the correlations in the first period of group A (n = 749). The middle four panels show the correlations using the mean values individually obtained more than 5 times over 3 years in group B (n = 369). The bottom four panels show the correlations in group B and non-diabetic group C (n = 62): Although linear relationships between G-gaps and GA/A1C ratios were calculated from the total data of groups B and C, the correlation depicted a cluster of group C of the non-diabetic siblings shown by (×) plots within a circle separate from a cluster of group B shown by dot (·) plots.

that the G-gap and the GA/A1C ratio are dependent, to a certain extent, on the A1C units of the designated comparison methods, such as A1C-NGSP. We first expected that the GA/A1C ratio would be a non-glycemic index similar to the G-gap proposed by Rodriguez-Segada *et al.* [7]. However, in the actual data with respect to the GA/A1C ratio, the GA/A1C-% ratio was affected 10.5% by A1C-NGSP and was significantly higher in the type 1 diabetes patients than in their BMI-comparable non-diabetic siblings. In contrast, the GA/A1C-SI ratio was significantly lower in the type 1 diabetes patients than in their siblings, being affected to a lesser degree, 1.4% by A1C-IFCC. The reason why the GA/A1C -% ratio was strongly affected by A1C-NGSP itself may be the presence of non-glycated hemoglobins in the underlying measurement systems [12, 13]. The higher the A1C-NGSP values, the lower are the corresponding GA/A1C -% ratios, given that the non-glycated content in A1C-NGSP may not increase in proportion to the corresponding GA value with increasing glycemic exposure.

The GA/A1C ratio may not be derivable from HbA1c by any simple conversion formula. Recently Cohen [32] pointed out an unexplained finding in the analyses by Selvin *et al.* [17] that there was a proportionately greater increase in GA and fructosamine concentrations than of A1C concentrations in the range of 5.4–5.8% in non-diabetic participants, apparent in the plots of GA and fructosamine versus A1C fitted with a nonlinear curve. By contrast, the relationships between A1C and both GA and fructosamine were linear within the diabetic population. A similar phenomenon was observed in the present study, revealing the relationship between GA/A1C-SI ratio and G-gap as a different cluster of the type 1 diabetes population from that of the non-diabetic population, as shown in the Fig. 2 group B and C panels. These findings suggest that GA/A1C-SI ratios must be determined as reference values in each population for the same race, age, disease, and disease type.

Still, our results indicate that the GA/A1C-SI ratio does not need adjustment and is highly correlated with the G-gap (Table 3 and Fig. 2). In contrast, the GA/A1C-% ratio needed adjustment by A1C-NGSP to show a high correlation with the corresponding G-gap, and would not be useful in regular practice.

As limitations of this study, both GA and the GA/A1C ratio are reported to be affected by diabetes type [19-22] and obesity [20, 22-24]. A similar tendency was also reported for the G-gap [6, 7]. In the stepwise analyses of the present study, the GA/A1C ratio was dependent to some extent on BMI, dose of insulin per weight, and duration of diabetes in addition to A1C. The effects of these parameters on the reference values of the GA/A1C ratio remain to be evaluated in each population. Of course, neither GA nor A1C values in disturbed metabolism should be included as reference values.

GA and fructosamine both reflect a weighted mean of blood glucose over the preceding 30 days [33], whereas A1C reflects a weighted mean over the preceding 100 days [34]. However, given that approximately 50% of A1C is produced during the 30–35 days prior to measurement, both GA and A1C are affected by any significant alteration in plasma glucose during this period. The GA/A1C ratio may thus reflect worsening or improving fluctuations in glycemic control over the short term [21, 22]. Some previous authors have argued that a high GA/A1C ratio is associated with postprandial glucose excursion, early progression to insulin therapy in type 2 diabetes, or other events [35, 36]. A high G-gap, corresponding to a low GA/A1C ratio in the present study, has been reported to be a predictive indicator of diabetic complications, especially diabetic nephropathy [3-5, 7]. These differences of high and low GA/A1C ratios in various clinical aspects may reflect the difference between pathological glycation of albumin and hemoglobin in the circulation and within the cell, respectively. This kind of study should take into consideration the individual intrinsic consistency of the GA/A1C-SI ratio over time.

Several studies have examined glycemic indexes with biological variation [37-43]. Deviations between mean blood glucose and A1C values with continuous glucose monitoring (CGM) have been shown to be consistent in each individual [39-41]. These deviations in mean blood glucose and the A1C value are called the glycohemoglobin index (GHI), and the biological variation of A1C has been examined [3, 4, 42, 43]. The G-gap is also reported to be an indicator with biological variation [5, 31], and Nayak *et al.* [6] reported that the G-gap has consistent biological variability in individuals. Recently, as mentioned above, fructosamine or GA and G-gap have been reported as predictive indicators for diabetic complications independent of A1C [16, 17, 32]. If the GA/A1C-SI ratio reflected the difference in biological variability of glycation between GA in the circulation and A1C within the cell, the GA/A1C-SI ratio might be a predictive indicator of diabetic complications accurately representing the G-gap. This potential remains to be investigated for the present